Correct(ed) Klett–Fernald algorithm for elastic aerosol backscatter retrievals: a sensitivity analysis

Johannes Speidel* and Hannes Vogelmann

Karlsruhe Institute of Technology (KIT), Institute of Meteorology and Climate Research Atmospheric Environmental Research (IMK-IFU), Campus Alpin, Garmisch-Partenkirchen, 82467, Germany
**Corresponding author: johannes.speidel@kit.edu*

Retrieval algorithms for aerosol elastic backscatter lidars are most commonly based on a signal inversion known as the Klett solution. While often used, a sign error in the original publication has barely been mentioned or recog-nized in the scientific community. In this study, we present a corrected Klett inversion and a sensitivity analysis of its implementation under different atmospheric conditions. We show that the error's dimension depends on multiple factors, thus preventing trivial *a posteriori* corrections on the results calculated with the original, uncorrected Klett solution. Comparing the uncorrected with the corrected Klett solution, long integration pathways in combination with low aerosol concentrations lead to substantial relative deviations of more than 100%, whereas short integra-tion pathways with high aerosol concentrations considerably reduce the relative deviations to magnitudes around 15%. The higher the altitude of layers with increased aerosol concentrations, the higher the deviations due to the incorrect usage of Klett's inversion, however on a slight level (≈ 1%).

1. INTRODUCTION

Aerosols are involved in multiple important processes that not only have a direct impact on air quality, but also influence cloud formation and the Earth's radiation budget [1]. Furthermore, observed composition and distribution of aerosols can deliver valuable information about atmospheric transport dynamics [2]. In addition, satellite-based atmospheric observations often need *a priori* information on aerosol optical depth. Therefore, it is important to obtain accurate measurements of the content and composition of aerosols in the atmosphere.

To measure the prevailing aerosol content in the atmosphere, elastic backscatter lidars are systems that are the most easy to implement and operate. Hence, even stratospheric measurements of aerosols were conducted shortly after the first lasers were constructed and employed into lidar systems in the early 1960s [3]. Since then, lidar aerosol observations have become an increasing focus of research, also for instrument calibrations of satellite systems (e.g., [4,5] and references therein). However, accurate measurements of aerosol's optical backscatter and extinction characteristics have been and still remain challenging.

This is due to the fact that the lidar equation [Eq. (1)] for elastic backscatter lidars is an underdetermined equation. Therefore, information on either the volume backscatter coefficient or the volume extinction coefficient has to be collected *a priori*, calling for additional observational data of one of those two. Several approaches to tackle this problem have been published, as, e.g., discussed in [6]. With his publication in 1972, Fernald presented a fundamental analytical approach to solve the lidar equation under the consideration of both molecular and particle signal contributions [7]. A major breakthrough in elastic backscatter signal processing was Klett's publication in 1981 [8], where, under the assumption of a power law relationship between volume backscatter and volume extinction coefficient, an analytical inversion solution to the lidar equation was developed. By reversing the bounds of integration, leading to an integration from high to low altitudes, this inversion algorithm proved to be mathematically stable without the need of additional measurements for lidar calibration. This solution, however, did not account for a molecular contribution in the lidar signal. Additional and equally important publications on the lidar signal inversion problem have been made by Fernald [9] and Sasano *et al*. [10]. The criticism on Klett's first solution contained therein was addressed in a follow-up publication by Klett in 1985. With this publication [11], Klett finalized the lidar inversion algorithm known as the "Klett–Fernald–Sasano algorithm." Therein, a finalized equation for the retrieval of aerosol backscatter coefficients under the consideration of molecular Rayleigh scattering is provided. Also, this inversion algorithm includes additional improvements with respect to variable backscatter-to-extinction ratios over height. However, due to his original idea of a backward integration scheme,

this inversion is most commonly simply referred to as Klett's solution.

By now, technologically more sophisticated lidar concepts have been developed, allowing for more accurate and versatile determination of aerosol properties, offering the advantage of more accurate results without *a priori* assumptions on the lidar ratio. Examples include high spectral resolution lidar (HSRL, [12]), or systems using Raman backscatter and combinations of multiple wavelengths (e.g., [13,14]). Nevertheless, despite its age and accompanying uncertainties, elastic backscatter coefficients measured with lidars, in some cases as a byproduct, still deliver valuable information on the atmospheric aerosol content and are therefore frequently used (e.g., [15–17]). For this purpose, Klett's inversion scheme still is a state-of-the-art method. However, Klett's renowned 1985 publication is afflicted by a sign error. This was first noticed by Kaestner in 1986, shortly after Klett's publication [18]. Nonetheless, based on the amount of citations, this important erratum has not gained its appropriate degree of recognition. In addition, there are indications that the sign error is still repeatedly adopted, presumably due to lacking knowledge of its existence. A very rare example in which the sign error is directly mentioned, though not explicitly explained, can be found in a publication of Zavyalov [19]. Fortunately, large parts both within literature and the lidar community have tacitly corrected the sign error (e.g., [20–25]). Unfortunately, error descriptions and clear guidance on how to properly use the inversion algorithm are lacking, which still leads to confusion. Interestingly, many publications simply state to use the lidar signal inversion according to Klett 1985 [11], without sharing the specific formula they were using, and without further comments on whether or not they have noticed the need for a correction of the original signs (e.g., [26–30]). Although a correct implementation can probably be assumed in most cases, the traceability is clearly affected. In conclusion, clear indications, descriptions, or even warnings of the sign error are hardly ever given. Moreover, in addition to the sign error itself, there are further complications and pitfalls regarding the correct usage of Klett's inversion algorithm. A detailed description of problems occurring in the inversion's implementation will be given in the following section. Given the unabated high relevance of Klett's 1985 algorithm [11] in the field of elastic backscatter lidars, the uncertainty regarding its possible incorrect implementation is so high that a certain degree of propagation of this error has to be assumed. Furthermore, the impact of using the wrong formulation of the Klett solution has never been discussed in quantitative terms. Therefore, this paper identifies at which point a sign error occurs in the original publication and presents a sign-corrected, stable solution derived from Klett's original inversion algorithm. To quantify the implication of the sign error on the inversion results, several case studies are carried out for multiple atmospheric conditions. This allows an estimation of how different measuring conditions are affected by varying intensities of aerosol load at multiple altitudes.

The mathematical details are described in Section 2, and the results of the quantitative case studies as well as their implications are discussed in Section 3. Finally, a brief summary is given in Section 4.

2. THEORY

This section focuses on a detailed derivation of Klett's solution and the point where a wrong sign was introduced in Klett's work [11]. As a result, we present a sign-corrected version of Eqs. (20) and (22) from the original publication. The crucial point we want to stress is the fact that the wrong sign is hidden in Klett's Eq. (20), serving as a substitute within his final Eq. (22). A detailed description of the corrected Klett solution is given in the development of our Eq. (9). Finally, the corrected equation is further transformed into a version without logarithmic terms, preventing numerical instabilities for profiles with very low aerosol content [Eq. (10)].

As stated in the Introduction, Klett's inversion from 1985 [11] is superior to the one he published in 1981 [8], as it specifically takes molecular Rayleigh scattering into account. Therefore, the improved 1985 Klett inversion should be used for calculating both backscatter and extinction coefficients, even though it is not always done that way (e.g., [31–33]).

The starting point for all considerations behind Klett's 1985 inversion is the well-known general lidar equation

$$P(r,\lambda) = C \cdot \beta(r,\lambda) \cdot \frac{1}{r^2} \cdot \exp\left[-2\int_0^r \alpha(r',\lambda)\mathrm{d}r'\right], \quad \textbf{(1)}$$

with P being the received power, C a lidar-dependent constant, r the range from the lidar, and β and α the volume backscatter and extinction coefficients, respectively. In addition, the equation is dependent on the wavelength λ at which the lidar is operated. For the sake of brevity, this dependence is omitted in the notation of the following equations but always has to be kept in mind. By introducing r_0 as a constant reference range and simplifying $S(r) = \ln(r^2 \cdot P(r))$, Klett [8] derives

$$S(r) - S_0 = \ln\frac{\beta(r)}{\beta_0} - 2\int_{r_0}^r \alpha(r')\mathrm{d}r', \quad \textbf{(2)}$$

where $S_0 = S(r_0)$ and $\beta_0 = \beta(r_0)$. This equation shows to be independent of the used lidar system. Deriving Eq. (2) by r then leads to

$$\frac{dS(r)}{dr} = \frac{1}{\beta(r)}\frac{d\beta(r)}{dr} - 2\alpha(r). \quad \textbf{(3)}$$

From this point on, within his 1985 publication, Klett introduces the lidar ratio B as a relation between backscatter and extinction coefficients in a way that

$$\beta(r) = \beta_P(r) + \beta_R(r) = B_P(r)\alpha_P(r) + B_R\alpha_R(r). \quad \textbf{(4)}$$

Subscript P denotes the particle contribution, whereas R stands for the molecular (Rayleigh) contribution on the backscatter and extinction coefficients. The molecular lidar ratio is constant over height with $B_R = \frac{3}{8\pi}\mathrm{sr}^{-1} \approx 0.119\,\mathrm{sr}^{-1}$. The particle lidar ratio, however, is capable of having variable values over height. If according *a priori* information is available, keeping $B_P(r)$ height dependent leads to improved results [11]. However, the values of $B_P(r)$ are most often chosen to have constant, height-independent values that best fit the prevailing atmospheric conditions (e.g., [34]). Inserting Eq. (4) into Eq. (3) then leads to the following:

$$\frac{dS(r)}{dr} = \frac{1}{\beta(r)}\frac{d\beta(r)}{dr} - 2\left(\frac{\beta_P(r)}{B_P(r)} + \frac{\beta_R(r)}{B_R}\right)$$
$$= \frac{1}{\beta(r)}\frac{d\beta(r)}{dr} - \frac{2\beta(r)}{B_P(r)} + 2\beta_R(r)\left(\frac{1}{B_P(r)} - \frac{1}{B_R}\right). \quad (5)$$

At this point, Klett introduces a new signal variable $S'(r)$ within the substitute $S' - S'_m$, analogous to Eq. (2). However, as can be seen in Eq. (21) in [11] and in Eq. (8) in this publication, this definition can raise confusion as there is no single variable S' but always the entire substitute $(S' - S'_m)(r)$. Therefore, we slightly modify the original notation and change the name of the substitute from $S'(r)$ to $S^*(r)$. Besides that, sticking to Klett's original notation, in the following, the index m always refers to the far-end reference range r_m so that, e.g., $S_m = S(r_m)$. The choice of the integration bounds results out of the important Klett 1981 publication [8], which led to improved mathematical stability of the inversion algorithm as the integration starts from the far end. At the introduction of the new signal variable $S^*(r)$ (called S' in [11]), a wrong sign was noted in the original publication [Eq. (20)]. Originally, the definition of the substitute $S^*(r)$ looks like this:

$$S^*(r) := (S' - S'_m)(r) = S(r) - S_m + \frac{2}{B_R}\int_r^{r_m} \beta_R(r')\mathrm{d}r'$$
$$- 2\int_r^{r_m} \frac{\beta_R(r')}{B_P(r')}\mathrm{d}r'$$
$$= S(r) - S_m + 2\int_r^{r_m}\left(\frac{1}{B_R} - \frac{1}{B_P(r')}\right)\beta_R(r')\mathrm{d}r', \quad (6)$$

while the correct substitute $S^*(r)$ should be

$$S^*(r) := (S' - S'_m)(r)$$
$$= S(r) - S_m - 2\int_r^{r_m}\left(\frac{1}{B_R} - \frac{1}{B_P(r')}\right)\beta_R(r')\mathrm{d}r'. \quad (7)$$

Here, it is very important to note that the error made in the introduction of $S^*(r)$ [Eq. (6)] would propagate into Eq. (9) and subsequently into the final Eq. (10), if not replaced by Eq. (7). Only if the sign-corrected $S^*(r)$ [Eq. (7)] is included does the following differential equation lead to the result of Eq. (21) intended by Klett [11]. Due to the reverse integration with the reference value at the upper end, signs have to be changed. This can be seen in the following differential:

$$\frac{dS^*(r)}{dr} = \frac{dS(r)}{dr} - \frac{2}{B_R}\frac{d}{dr}\int_r^{r_m}\beta_R(r')\mathrm{d}r' + 2\frac{d}{dr}\int_r^{r_m}\frac{\beta_R(r')}{B_P(r')}\mathrm{d}r'$$
$$= \frac{dS(r)}{dr} + 2\frac{\beta_R(r)}{B_R} - 2\frac{\beta_R(r)}{B_P(r)}$$
$$= \frac{1}{\beta(r)}\frac{d\beta(r)}{dr} - 2\frac{\beta_R(r)}{B_P(r)} - 2\frac{\beta_P(r)}{B_P(r)} + 2\frac{\beta_R(r)}{B_P(r)}$$
$$- 2\frac{\beta_R(r)}{B_R} + 2\frac{\beta_R(r)}{B_R} - 2\frac{\beta_R(r)}{B_P(r)}$$
$$= \frac{1}{\beta(r)}\frac{d\beta(r)}{dr} - 2\frac{\beta(r)}{B_P(r)}.$$

Subsequently, volume backscatter coefficients can be calculated as follows:

$$\beta(r) = \frac{\exp(S' - S'_m)}{\frac{1}{\beta_m} + 2\int_r^{r_m}\frac{\exp(S' - S'_m)\mathrm{d}r'}{B_P(r')}}. \quad (9)$$

For easier comparability with the original Eq. (22) in [11], we kept the notation $S' - S'_m$, which we introduced as $S^*(r) = (S' - S'_m)(r)$ earlier. As can be seen, Eq. (9) is actually identical in its notation with Eq. (22) from Klett 1985 [11]. However, it is very important to recognize that our Eq. (9) refers to the substitute $S^*(r)$, which is now defined with correct signs [Eq. (7)]. We emphasize that typos can be found in many manuscripts and that such faults in the final prints do not always have to coincide with the actual, implemented method. However, wrong equations with the original sign error from [11] are occasionally published (e.g., [35–37]). In addition, another sign error in the denominator, which cannot unambiguously be assigned to the original sign confusion around Klett's 1985 publication, has been used as well (e.g., [38,39]). Therefore, we see a double check of the used inversion algorithm and all published equations on this error as essential to prevent its further propagation. In spite of the corrected sign error, one major drawback of Eq. (9) is the asymmetry of the logarithm in the definition of the signal variable $S(r) = \ln(r^2 P(r))$, leading to strong signal variations or even undefined values if the noisy signal values draw near zero. This implies filtering or substitution of all values $P(r) \leq 0$. Criticism on the use of the logarithm has already been voiced by, e.g., [38] in 1995. Nevertheless, there are still examples in which the logarithm is used (e.g., [40,41]). In addition to this issue, the logarithmic term can often be found in equations that refer to Klett 1985 [11], but completely misinterpret the substitute $S^*(r)$ from Eq. (7) in a way that it is falsely assumed to be simply $S^*(r) = S(r) - S_m$ (e.g., [42–48]). To avoid these problems, we recommend using a transformed formulation without a logarithm:

$$\beta(r) = \frac{\hat{S}(r)\cdot\exp[Y(r)]}{\frac{\hat{S}_m}{\beta_m} + 2\int_r^{r_m}\frac{\hat{S}(r')}{B_P(r')}\cdot\exp[Y(r')]\mathrm{d}r'}, \quad (10)$$

with

$$Y(r) = -2\int_r^{r_m}\left(\frac{1}{B_R} - \frac{1}{B_P(r')}\right)\beta_R(r')\mathrm{d}r',$$

$$\hat{S}(r) = r^2 P(r).$$

This notation can easily be derived from Eq. (9) by consequently applying the exponential function on the logarithmic terms $S(r)$ and S_m in the substitute $S^*(r)$. If one considers $B_P(r') = B_P$ as being constant over height, this formula equals the solution proposed by Fernald [9], which was published before Klett's publication in 1985 [11]. Here, Eq. (10) is free of the sign error hidden in Eqs. (20) and (22) of Klett's 1985 work and takes into account the possibility for variable $B_P(r')$. This, or similar notations are well established (e.g., [10,25]). We recommend using this formulation [Eq. (10)] for elastic backscatter inversions if applying Klett's original 1985 algorithm.

3. SENSITIVITY STUDY

After analytically correcting the sign error in Klett's original publication, its impact under differing atmospheric conditions is not self-evident by looking only at the equation. Therefore, in the following, the error caused by a wrong sign within Klett's substitution in the inversion algorithm is examined with the use of both artificial and real lidar signals in varying atmospheric conditions. With this, a classification on whether this error has to be considered marginal can be achieved. To further simplify the case study, all examples presented in this section are considered to be free of any overlap function. Furthermore, the particle lidar ratio is kept constant for all case studies such that $B_P(r) = B_P = 1/50\ \mathrm{sr}^{-1}$. Also, all case studies assume the presence of optically relevant molecules, meaning that $\beta_R(r) \neq 0$. In cases in which $\beta_R(r) = 0$ (dust load in space in absence of a gaseous atmosphere), the sign error does not affect the results as can be seen from Eqs. (7) and (10).

A. Case Study with No Aerosol Load

In the first case, a simplified atmosphere with no aerosol content is assumed. For this case, an artificial lidar return signal is generated [based on Eq. (1)], solely influenced by the molecular Rayleigh backscatter derived from a U.S. standard atmosphere [49]. For this first, aerosol-free condition, the lidar is assumed to be situated at sea level. As the Klett inversion algorithm is basically an integration over height, a long integration path is chosen with an arbitrary reference height at 2000 bin(1 bin $\hat{=}$ 7.5 m), i.e., at an altitude of 15 km above sea level (ASL).

While the correct implementation of Klett's inversion results in the expected $\beta_P(r) = 0$ over the entire range, it can be demonstrated that the uncorrected usage with the wrong sign therein causes negative values of β_P (Fig. 1). Those values magnify continuously in the negative range the closer we get from high altitudes to the ground, reaching values $\beta_P < -3 \cdot 10^{-7}\ (\mathrm{m \cdot sr})^{-1}$. Under realistic tropospheric conditions at such altitudes, β_P regularly exceeds much higher values of the order of magnitude $+10^{-5}\ (\mathrm{m \cdot sr})^{-1}$. The error obtained from this specific case study can thus be assumed marginal for typical tropospheric conditions.

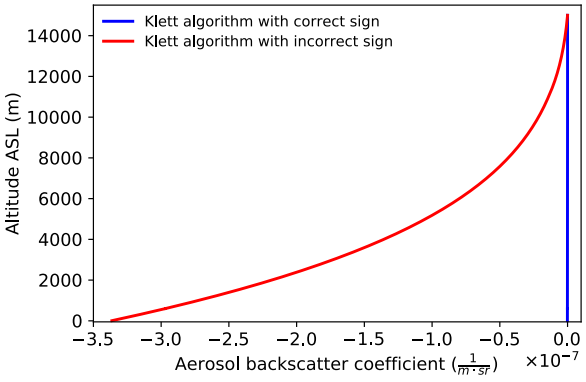

Fig. 1. Aerosol backscatter coefficients, calculated with the corrected inversion equation (blue) and with the incorrect sign therein (red).

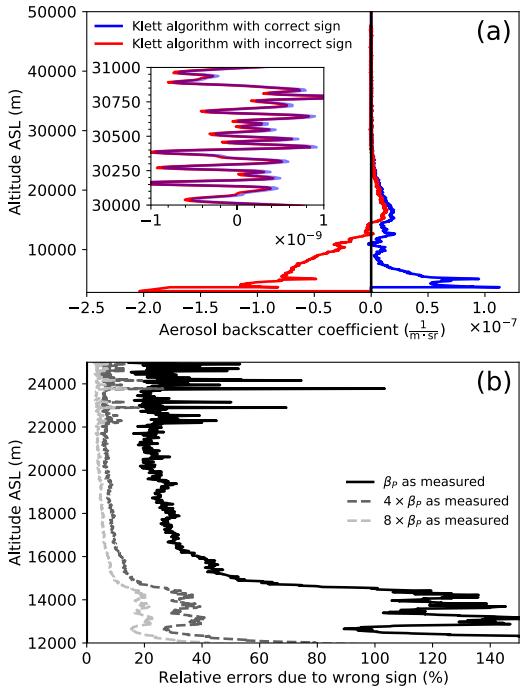

Fig. 2. (a) (Un)corrected Klett inversion of aerosol backscatter coefficients on the basis of a representative profile measured on Mount Zugspitze, Germany. The calculated aerosol backscatter coefficients at high altitudes are enlarged in the inset for better visibility. (b) shows relative errors due to the incorrect usage with the wrong sign for a selected range of altitude.

B. Case Study with Low Aerosol Load

To assess the sign problem in realistic surroundings with low aerosol load, the second case is based on actual aerosol measurements from a ground-based lidar. At an altitude of 2675 m ASL, the Garmisch–Partenkirchen aerosol lidar provides one of the longest time series of stratospheric aerosol measurements [15]. We selected a characteristic profile from January 2022 as representative for the case of an elevated lidar, located above the planetary boundary layer and with the capability of reaching high into the stratosphere. In this case, measurements reach a height of over 46 km ASL, which corresponds to roughly 5800 bins or 43.5 km above the lidar site. As previously, the measured values of β_P are again used to create an artificial lidar return signal. As the Klett algorithm in the presented form assumes the reference height to be free of aerosols, we set $\beta_P(r_m) = 0$. This is true for all presented case studies. Analogous to the aerosol-free condition, using the uncorrected inversion in this scenario results in smaller values for β_P, as displayed in Fig. 2(a). Again, the negative bias amplifies towards lower altitudes (and with a longer integration pathway, respectively), leading to negative values. Note that besides the fact that the integration length is almost three times as long as in the previous scenario, the values from the lowest layers are still bigger than those from the aerosol-free scenario. But still, the relative deviations between the corrected and uncorrected results are very high [Fig. 2(b)]. The lowest values are around 20%, whereas the highest values by far exceed 100%, especially

below the altitudes shown in this plot. Interestingly, Fig. 2(b) also shows that the discrepancies are getting remarkably smaller by only increasing the aerosol content with constant factors. Nevertheless, considering the clear negative signal, the usage of the wrong algorithm under such atmospheric conditions would immediately lead to a questioning of one's own algorithm implementation. Therefore, in this case, the error can be seen as substantial. However, in cases of solely observing the stratosphere with an enhanced dust load, this might be overseen and lead to misinterpretation of measurement results.

C. Case Study with High Aerosol Load

To account for the presented effect of a decrease of the relative errors with higher aerosol loads, the third and last case study is set to a lidar situated within the planetary boundary layer. Again, we used measured values of β_P, in this case from measurements performed with a HSRL system. The measurement was performed within the CHEESEHEAD campaign [50] during the summer of 2019 in northern Wisconsin, USA. Contrasting the site at Mount Zugspitze, the instrument was standing at an altitude of ≈400 m ASL, within the planetary boundary layer. To demonstrate the effect for high aerosol concentrations, we selected a profile from a time period with a high aerosol load. However, it has to be stressed that no major human aerosol source was existent in proximity of this remote site. Concerning measurements within the boundary layer, higher values of β_P are commonly observed at other measurement sites. Yet, the maximum values of β_P are two orders of magnitude higher than those at Mount Zugspitze [Fig. 3(a)]. In contrast to the formerly shown cases, here, the aerosol backscatter coefficients do not reveal the usage of an incorrect algorithm as they do not turn into negative values. Additionally, the relative deviations between the implementation of the corrected and uncorrected inversions become smaller, with a maximum of about 25% (integration pathway: ≈ 16 km). Considering the occurrence of higher aerosol concentrations, those relative discrepancies can become even less [Fig. 3(c)]. As already indicated, the incorrect usage of the inversion should have a magnifying effect on the error, which correlates with the length of the integration path. This becomes evident in Fig. 3(d), where the reference altitude is defined to be half the distance (≈8 km instead of ≈ 16 km). Given that aerosol concentrations in each height stay the same, the relative deviations are now substantially smaller, with maximum values of about 18%. The higher the aerosol concentrations, the further the drop in differences between implementations of the corrected and uncorrected inversion algorithms. When even system inter-comparison studies result in deviations of 10% or less, one might hardly question the inversion algorithm but assume a system offset instead. By analyzing the relative deviations, we observe that high aerosol loads remarkably reduce the differences. For example, for the intense aerosol peak above 3 km, a simultaneous drop within the relative deviations can be observed. Regarding the absolute deviations, however, results show a different picture in two regards. First, aerosol peaks show higher absolute discrepancies. Second, and as a consequence of this, overall elevated aerosol concentrations increase the absolute deviations, too [Fig. 3(b)].

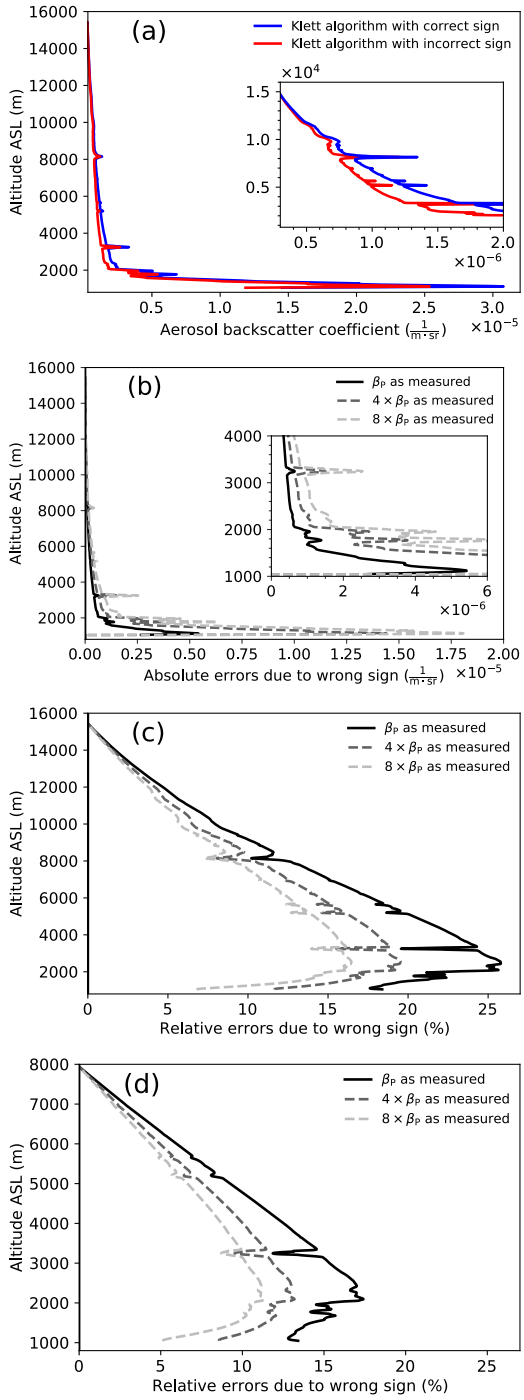

Fig. 3. (a) (Un)corrected Klett inversion of aerosol backscatter coefficients on the basis of a representative profile measured in northern Wisconsin, USA. The calculated aerosol backscatter coefficients at high altitudes are enlarged in the inset for better visibility. (b) Absolute errors are compared with (c) relative errors. (d) Relative errors are also shown for the case of the integration path length being halved. (a), (b) Enlarged insets ease the interpretation of the calculated results for specific altitudes.

As a last step, we focus on the question of how the incorrect usage of the inversion with the wrong sign therein affects the resulting backscatter coefficients, depending on aerosol layers at different altitudes. Therefore, we assumed a scenario in which

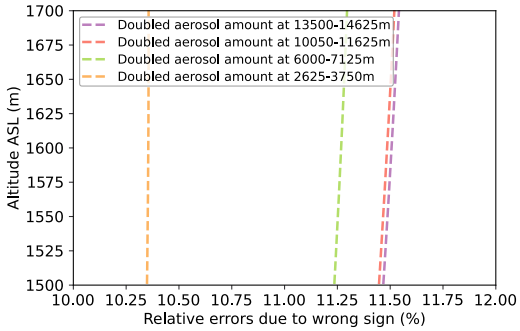

Fig. 4. Relative errors induced by the incorrect usage of Klett's inversion for additional aerosol layers sharply defined within a range of 150 bin, introduced in different altitudes.

the vertical distribution of β_R is again based on the U.S. standard atmosphere. To be independent of any natural structures with enhanced aerosol in real data, we then added an artificial vertical aerosol distribution with an exponential decrease over height. The function parameters are chosen such that the afterwards retrieved values of β_P were within the same value range as for the previously shown HSRL measurements. Finally, aerosol steps with a vertical extent of 150 bins are introduced at different altitudes. The increase of aerosol is set to always twice as much as the aerosol backscatter coefficients at every single bin within the aerosol layer. This artificial signal is retrieved with the reference altitude $r_m \approx 16$ km, analogous to the previously shown CHEESEHEAD example. We find that the relative errors due to incorrect usage of the inversion turn out to be lower, the lower we assumed the altitude of the increased aerosol layer (Fig. 4). This also applies if the additional aerosol amount that is added to the aerosol backscatter coefficients is supposed to always be the same. For absolute errors, the trend of deviations is similar. Although shown for only a specific height, those results apply for all altitudes below the additionally introduced aerosol layer as well.

In conclusion, for boundary layer lidars, the deviations resulting from the wrong implementation with the sign error are much smaller than in the previously shown scenario. Nevertheless, they are still substantial and cannot be assumed to be marginal. But they can easily end up in misleading results because the retrieved β_P profiles are still within a realistic bandwidth, and the deviations are not obvious (such as negative values).

4. SUMMARY AND CONCLUSION

We identified and reviewed scientific literature for a sign error within the original publication of the Klett inversion from 1985 [11], which is widely used in the field of elastic backscatter lidars. The correct(ed) version of Klett's solution has been presented as Eq. (10), which we advise to use. With the notation shown here, Eq. (10) contains a slight improvement towards Klett's original solution, as it does not contain any asymmetric logarithmic terms that cause problems with noisy data close to zero. For a constant lidar ratio of aerosols (β_P/α_P), this equation was shown to be identical to the proposed solution by Fernald in 1984 [9], which is correct, but not always referenced.

In a sensitivity analysis, three differing atmospheric case studies were carried out, which narrowed down the error's behavior for different lidar setups. Generally, the incorrect usage of Klett's inversion with the sign error therein was shown to lead to an underestimation of the aerosol backscatter coefficients β_P, resulting in even negative values in cases of a very low aerosol load (e.g., stratosphere). For an artificial atmosphere without any aerosols, values of $\beta_P \sim -10^{-7}(\mathrm{m}\cdot\mathrm{sr})^{-1}$ were calculated instead of the expected values $\beta_P = 0$. When simulating typical conditions for stratospheric lidars with long integration pathways and little aerosol content, the underestimation of β_P builds up the lower the altitude gets. With an integration pathway of roughly 43.5 km, the deviations of results, calculated with the corrected and uncorrected Klett inversions, exceeded values of 100% by far.

Assuming realistic boundary layer conditions with enhanced aerosol content revealed overall smaller relative deviations compared to the aerosol-depleted stratospheric conditions. Maximum discrepancies of $\geq$25% occurred for an integration pathway of 15 km. Halving the integration pathway reduced maximum deviations to values of $\geq$17%, exhibiting an error dependency on the integration length. Further increases of the aerosol load (by a multiplied, constant factor of four and an integration length of over 15 km) led, in maximum, to a reduction of deviations of more than 6% for the long integration pathway and a reduction of more than 4% for a halved pathway. The absolute errors, however, increased with higher aerosol concentrations. Without any factorial multiplication of aerosol load, the calculated absolute errors peaked at values of $\geq 0.5\cdot 10^{-5}\,(\mathrm{m}\cdot\mathrm{sr})^{-1}$. With the same factorial multiplication of four, the absolute errors reached values of $\geq 1.4\cdot 10^{-5}\,(\mathrm{m}\cdot\mathrm{sr})^{-1}$. In a last step, we have shown that the error's magnitude is dependent on the height in which aerosol layers are present. The errors made by the incorrect usage of Klett's inversion in the retrieval were bigger, the higher the aerosol layer was. This was true for both relative and absolute discrepancies. However, differences were marginal. In the exemplary scenario, the relative deviations differed by over 1% at overall values of $\approx$ 11%.

Overall, we have demonstrated that the error caused by the incorrect implementation of Klett's inversion with the wrong sign therein is dependent on multiple factors: aerosol concentration, altitude of aerosol occurrence, and the length of the integration pathway. Simple *a posteriori* corrections on miscalculated data are therefore hardly possible. The error magnitude is substantial for stratospheric lidars based above the planetary boundary layer. For boundary layer lidars, the errors are significantly smaller, potentially preventing their detection. In conclusion, the errors caused by the wrong sign in the Klett inversion algorithm may be unnoticed in boundary layer elastic aerosol retrievals, but still are too big to be negligible. Our study contributes to a better understanding of the implementation of the Klett algorithm for elastic backscatter aerosol retrievals and proposes an improved, sign-corrected solution as best practice.

Funding. Deutsche Forschungsgemeinschaft (406980118, VO2423/1-1); Karlsruhe Institute of Technology.

Acknowledgment. First and foremost, we cordially thank Dr. James Klett for his impartial endorsement as well as his additional remarks during the

review process of this paper. This led to significant improvements. In addition, we highly appreciate the support from both Prof. Dr. Hans Peter Schmid and PD Dr. Ralf Sussmann. Also, we thank Dr. Thomas Trickl, who confirmed and supported our initial considerations, as well as Matthias Perfahl for his technical support. Also, we thank the University of Wisconsin Lidar Group for sharing their data from the CHEESEHEAD campaign. Finally, we thank Karina Winkler for her conscientious proofreading.

Disclosures. The authors declare no conflicts of interest.

Data availability. Data underlying the results presented in this paper are not publicly available at this time but may be obtained from the authors upon reasonable request.

REFERENCES

1. P. Forster, T. Storelvmo, K. Armour, W. Collins, J.-L. Dufresne, D. Frame, D. Lunt, T. Mauritsen, M. Palmer, M. Watanabe, M. Wild, and H. Zhang, "The earth's energy budget, climate feedbacks, and climate sensitivity," in *Climate Change 2021: The Physical Science Basis. Contribution of Working Group I to the Sixth Assessment Report of the Intergovernmental Panel on Climate Change*, V. Masson-Delmotte, P. Zhai, A. Pirani, S. Connors, C. Péan, S. Berger, N. Caud, Y. Chen, L. Goldfarb, M. Gomis, M. Huang, K. Leitzell, E. Lonnoy, J. Matthews, T. Maycock, T. Waterfield, O. Yelekçi, R. Yu, and B. Zhou, eds. (Cambridge University, 2021), pp. 923–1054.
2. S. Kremser, L. W. Thomason, M. von Hobe, *et al.*, "Stratospheric aerosol - observations, processes, and impact on climate," Rev. Geophys. **54**, 278–335 (2016).
3. G. Fiocco and G. Grams, "Observations of the aerosol layer at 20 km by optical radar," J. Atmos. Sci. **21**, 323–324 (1964).
4. G. L. Schuster, M. Vaughan, D. MacDonnell, W. Su, D. Winker, O. Dubovik, T. Lapyonok, and C. Trepte, "Comparison of CALIPSO aerosol optical depth retrievals to AERONET measurements, and a climatology for the lidar ratio of dust," Atmos. Chem. Phys. **12**, 7431–7452 (2012).
5. A. Comerón, C. Muñoz-Porcar, F. Rocadenbosch, A. Rodríguez-Gómez, and M. Sicard, "Current research in lidar technology used for the remote sensing of atmospheric aerosols," Sensors **17**, 1450 (2017).
6. R. T. H. Collis and P. B. Russell, "Lidar measurement of particles and gases by elastic backscattering and differential absorption," in *Laser Monitoring of the Atmosphere*, E. D. Hinkley, ed. (Springer Berlin Heidelberg, 1976), pp. 71–151.
7. F. G. Fernald, B. M. Herman, and J. A. Reagan, "Determination of aerosol height distributions by lidar," J. Appl. Meteorol. Climatol. **11**, 482–489 (1972).
8. J. D. Klett, "Stable analytical inversion solution for processing lidar returns," Appl. Opt. **20**, 211–220 (1981).
9. F. G. Fernald, "Analysis of atmospheric lidar observations: some comments," Appl. Opt. **23**, 652–653 (1984).
10. Y. Sasano, E. V. Browell, and S. Ismail, "Error caused by using a constant extinction/backscattering ratio in the lidar solution," Appl. Opt. **24**, 3929–3932 (1985).
11. J. D. Klett, "Lidar inversion with variable backscatter/extinction ratios," Appl. Opt. **24**, 1638–1643 (1985).
12. E. E. Eloranta, "High spectral resolution lidar," in *Lidar: Range-Resolved Optical Remote Sensing of the Atmosphere*, C. Weitkamp, ed. (Springer New York, 2005), pp. 143–163.
13. J. Reichardt, U. Wandinger, V. Klein, I. Mattis, B. Hilber, and R. Begbie, "RAMSES: German Meteorological Service autonomous Raman lidar for water vapor, temperature, aerosol, and cloud measurements," Appl. Opt. **51**, 8111–8131 (2012).
14. D. Althausen, R. Engelmann, H. Baars, B. Heese, A. Ansmann, D. Müller, and M. Komppula, "Portable Raman lidar PollyXT for automated profiling of aerosol backscatter, extinction, and depolarization," J. Atmos. Ocean. Technol. **26**, 2366–2378 (2009).
15. T. Trickl, H. Giehl, H. Jäger, and H. Vogelmann, "35 yr of stratospheric aerosol measurements at Garmisch-Partenkirchen: from Fuego to Eyjafjallajökull, and beyond," Atmos. Chem. Phys. **13**, 5205–5225 (2013).
16. G. Pappalardo, A. Amodeo, A. Apituley, A. Comeron, V. Freudenthaler, H. Linné, A. Ansmann, J. Bösenberg, G. D'Amico, I. Mattis, L. Mona, U. Wandinger, V. Amiridis, L. Alados-Arboledas, D. Nicolae, and M. Wiegner, "EARLINET: towards an advanced sustainable European aerosol lidar network," Atmos. Meas. Tech. **7**, 2389–2409 (2014).
17. S. M. Khaykin, S. Godin-Beekmann, P. Keckhut, A. Hauchecorne, J. Jumelet, J.-P. Vernier, A. Bourassa, D. A. Degenstein, L. A. Rieger, C. Bingen, F. Vanhellemont, C. Robert, M. DeLand, and P. K. Bhartia, "Variability and evolution of the midlatitude stratospheric \ hack\ break aerosol budget from 22 years of ground-based lidar and satellite observations," Atmos. Chem. Phys. **17**, 1829–1845 (2017).
18. M. Kaestner, "Lidar inversion with variable backscatter/extinction ratios: comment," Appl. Opt. **25**, 833–835 (1986).
19. V. V. Zavyalov, C. Marchant, G. E. Bingham, T. D. Wilkerson, J. L. Hatfield, R. S. Martin, P. J. Silva, K. D. Moore, J. A. Swasey, D. J. Ahlstrom, and T. Jones, "Aglite lidar: calibration and retrievals of well characterized aerosols from agricultural operations using a three-wavelength elastic lidar," J. Appl. Remote Sens. **3**, 033522 (2009).
20. V. A. Kovalev, *Solutions in LIDAR Profiling of the Atmosphere* (Wiley, 2015).
21. A. Ansmann and D. Müller, "Lidar and atmospheric aerosol particles," in *Lidar: Range-Resolved Optical Remote Sensing of the Atmosphere*, C. Weitkamp, ed. (Springer New York, 2005), pp. 105–141.
22. V. Matthias, V. Freudenthaler, A. Amodeo, *et al.*, "Aerosol lidar intercomparison in the framework of the EARLINET project. 1.Instruments," Appl. Opt. **43**, 961–976 (2004).
23. M. Sicard, F. Molero, J. L. Guerrero-Rascado, R. Pedros, F. J. Exposito, C. Cordoba-Jabonero, J. M. Bolarin, A. Comeron, F. Rocadenbosch, M. Pujadas, L. Alados-Arboledas, J. A. Martinez-Lozano, J. P. Diaz, M. Gil, A. Requena, F. Navas-Guzman, and J. M. Moreno, "Aerosol lidar intercomparison in the framework of SPALINET—the Spanish lidar network: methodology and results," IEEE Trans. Geosci. Remote Sens. **47**, 3547–3559 (2009).
24. P. Chazette, "The monsoon aerosol extinction properties at Goa during INDOEX as measured with lidar," J. Geophys. Res. Atmos. **108**, 4187 (2003).
25. H. Eisele and T. Trickl, "Improvements of the aerosol algorithm in ozone lidar data processing by use of evolutionary strategies," Appl. Opt. **44**, 2638–2651 (2005).
26. A. Dörnbrack, T. Birner, A. Fix, H. Flentje, A. Meister, H. Schmid, E. V. Browell, and M. J. Mahoney, "Evidence for inertia gravity waves forming polar stratospheric clouds over Scandinavia," J. Geophys. Res. Atmos. **107**, SOL 30-1–SOL 30-18 (2002).
27. Q. Hu, P. Goloub, I. Veselovskii, J.-A. Bravo-Aranda, I. E. Popovici, T. Podvin, M. Haeffelin, A. Lopatin, O. Dubovik, C. Pietras, X. Huang, B. Torres, and C. Chen, "Long-range-transported Canadian smoke plumes in the lower stratosphere over northern France," Atmos. Chem. Phys. **19**, 1173–1193 (2019).
28. D. Müller, F. Wagner, U. Wandinger, A. Ansmann, M. Wendisch, D. Althausen, and W. von Hoyningen-Huene, "Microphysical particle parameters from extinction and backscatter lidar data by inversion with regularization: experiment," Appl. Opt. **39**, 1879–1892 (2000).
29. E. Barbaro, J. V.-G. de Arellano, H. G. Ouwersloot, J. S. Schröter, D. P. Donovan, and M. C. Krol, "Aerosols in the convective boundary layer: shortwave radiation effects on the coupled land-atmosphere system," J. Geophys. Res. Atmos. **119**, 5845–5863 (2014).
30. B. I. Vasil'ev and O. Mannoun, "IR differential-absorption lidars for ecological monitoring of the environment," Quantum Electron. **36**, 801 (2006).
31. D. Yuan, Z. Mao, P. Chen, Y. He, and D. Pan, "Remote sensing of seawater optical properties and the subsurface phytoplankton layer in coastal waters using an airborne multiwavelength polarimetric ocean lidar," Opt. Express **30**, 29564–29583 (2022).
32. L. Mei, P. Guan, Y. Yang, and Z. Kong, "Atmospheric extinction coefficient retrieval and validation for the single-band Mie-scattering Scheimpflug lidar technique," Opt. Express **25**, A628–A638 (2017).
33. P. A. Lewandowski, W. E. Eichinger, H. Holder, J. Prueger, J. Wang, and L. I. Kleinman, "Vertical distribution of aerosols in the vicinity of

Mexico City during MILAGRO-2006 Campaign," Atmos. Chem. Phys. **10**, 1017–1030 (2010).
34. J. Ackermann, "The extinction-to-backscatter ratio of tropospheric aerosol: a numerical study," J. Atmos. Ocean. Technol. **15**, 1043–1050 (1998).
35. J. Kasparian, E. Frejafon, P. Rambaldi, J. Yu, B. Vezin, J. P. Wolf, P. Ritter, and P. Viscardi, "Characterization of urban aerosols using SEM-microscopy, x-ray analysis and lidar measurements," Atmos. Environ. **32**, 2957–2967 (1998).
36. M. Adam, M. Pahlow, V. A. Kovalev, J. M. Ondov, M. B. Parlange, and N. Nair, "Aerosol optical characterization by nephelometer and lidar: the Baltimore Supersite experiment during the Canadian forest fire smoke intrusion," J. Geophys. Res. Atmos. **109**, D16S02 (2004).
37. P. Hegde, P. Pant, and Y. Bhavani Kumar, "An integrated analysis of lidar observations in association with optical properties of aerosols from a high altitude location in central Himalayas," Atmos. Sci. Lett. **10**, 48–57 (2009).
38. S. A. Young, "Analysis of lidar backscatter profiles in optically thin clouds," Appl. Opt. **34**, 7019–7031 (1995).
39. E. Montilla-Rosero, A. Silva, C. Jimenez, R. Hernandez, and C. Saavedra, "Optical characterization of lower tropospheric aerosols by the Southern East Pacific Lidar Station (Concepcion, Chile)," J. Aerosol Sci. **92**, 16–26 (2016).
40. A. Pantazis and A. Papayannis, "Lidar algorithms and technique in 3D scanning for planetary boundary layer height and single-beam-single-pointing wind speed retrieval," Appl. Opt. **58**, 2284–2293 (2019).
41. A. Pantazis, A. Papayannis, and G. Georgousis, "Lidar algorithms in 3D scanning for atmospheric layering and planetary boundary layer height retrieval: comparison with other techniques," Appl. Opt. **57**, 8199–8211 (2018).
42. A. Ananthavel, S. K. Mehta, S. Ali, T. V. R. Reddy, V. Annamalai, and D. N. Rao, "Micro pulse lidar measurements in coincidence with CALIPSO overpasses: Comparison of tropospheric aerosols over Kattankulathur (12.82oN, 80.04oE)," Atmos. Pollut. Res. **12**, 101082 (2021)..
43. A. Ananthavel, S. K. Mehta, T. V. R. Reddy, S. Ali, and D. N. Rao, "Vertical distributions and columnar properties of the aerosols during different seasons over Kattankulathur (12.82oN, 80.04oE): a semi-urban tropical coastal station," Atmos. Environ. **256**, 118457 (2021).
44. R. Rossi, M. Gelfusa, A. Malizia, and P. Gaudio, "Adaptive quasi-unsupervised detection of smoke plume by LiDAR," Sensors **20**, 6602 (2020).
45. H. Liu and Z. Wang, "An iterative calibrating method for airborne atmospheric detection lidar based on the Klett forward integral equation," Opt. Commun. **452**, 476–480 (2019).
46. P. Kulkarni and S. Ramachandran, "Comparison of aerosol extinction between lidar and SAGE II over Gadanki, a tropical station in India," Ann. Geophys. **33**, 351–362 (2015).
47. P. Kulkarni, S. Ramachandran, Y. Bhavani Kumar, D. Narayana Rao, and M. Krishnaiah, "Features of upper troposphere and lower stratosphere aerosols observed by lidar over Gadanki, a tropical Indian station," J. Geophys. Res. Atmos. **113**, D17207 (2008).
48. A. Jayaraman, S. Ramachandran, Y. B. Acharya, and B. H. Subbaraya, "Pinatubo volcanic aerosol layer decay observed at Ahmedabad (23N), India, using neodymium:yttrium/aluminium/garnet backscatter lidar," J. Geophys. Res. Atmos. **100**, 23209–23214 (1995).
49. ICAO (International Civil Aviation Organization), *Manual of the ICAO Standard Atmosphere: Extended to 80 Kilometres (262 500 Feet)*, 3rd ed. (1993).
50. B. J. Butterworth, A. R. Desai, P. A. Townsend, *et al.*, "Connecting Land–Atmosphere Interactions to Surface Heterogeneity in CHEESEHEAD19," Bull. Am. Meteorol. Soc. **102**(2), E421–E445 (2021).